

Catalytic Hydroarylation of Olefins Promoted by Dicationic Platinum(II) and Palladium(II) Complexes. The Interplay of C–C Bond Formation and M–C Bond Cleavage

Maria Elena Cucciolito, Angela D'Amora, Angela Tuzi, and Aldo Vitagliano*

Dipartimento di Chimica "Paolo Corradini", Università di Napoli "Federico II",
Complesso Universitario di Monte S. Angelo, Via Cintia, I 80126 Napoli, Italy

Received July 11, 2007

The coordinated olefin in dicationic platinum(II) and palladium(II) complexes $[M(\text{PNP})(\text{olefin})](\text{SbF}_6)_2$ ($M = \text{Pt}, \text{Pd}$; $\text{PNP} = 2,6\text{-bis}(\text{diphenylphosphinomethyl})\text{pyridine}$; olefin = ethene, propene) is electrophilic enough to react with benzene rings activated by methoxy substituents. If the proton released by the aromatic ring is trapped by a base, stable σ -alkyl derivatives of the type $[M(\text{PNP})\text{CH}_2\text{CH}(\text{R})\text{Ar}](\text{SbF}_6)$ or $[M(\text{PNP})\text{CH}(\text{R})\text{CH}_2\text{Ar}](\text{SbF}_6)$ ($\text{R} = \text{H}, \text{Me}$) are formed; otherwise the $\text{M}-\text{C}$ σ -bond can be cleaved by the proton, setting up a catalytic cycle that leads to the alkylated aromatic compound. The molecular structure of the σ -alkyl derivative $[(\text{PNP})\text{PtCH}_2\text{CH}_2-\text{C}_6\text{H}_2(\text{OMe})_3](\text{BF}_4)$ has been determined by X-ray diffraction analysis, and the factors affecting the mechanism and the rates of the catalytic reaction have been qualitatively investigated and rationalized, showing that the rates of C–C bond formation and M–C bond cleavage are inversely correlated.

Introduction

The electrophilic activation of unsaturated substrates by coordination to a transition metal ion is a very remarkable phenomenon, which is found at the core of most relevant metal-catalyzed processes.¹ As could be intuitively anticipated, there is also wide experimental² and theoretical³ evidence that the electrophilicity of the coordinated alkene can be enhanced by increasing the positive charge on the metal ion. For example, dicationic Pt(II) and Pd(II) olefin complexes easily undergo the nucleophilic attack of aromatic amines such as chloroanilines,^{4,5} while the neutral species need the more basic aliphatic amines to react.⁶

The primary product of a nucleophilic attack is a $\text{M}-\text{C}$ σ -bonded species, whose successive fate depends on the kind of nucleophile carrying on the attack. We recently found that when the coordinated olefin is strongly activated, as in dicationic complexes of the tridentate pincer ligand 2,6-bis(diphenylphosphinomethyl)pyridine (PNP), the attack can be carried out by a bonding π -electron pair of an electron-rich olefin.⁷ In this case an electron vacancy is left on the adjacent carbon atom and a carbocation is formed as an intermediate. The successive

rearrangement of the carbocation can result in the cleavage of the metal–carbon σ -bond, thus making a coordination site available to a further olefin molecule and opening the way to a catalytic process (Scheme 1). More usually, the attack can be carried out by a nonbonding lone pair on a heteroatom such as nitrogen. In this case no electron vacancy is produced, and the positive charge rests on the heteroatom. If the heteroatom brings a proton, this becomes acidic and could in principle cleave the $\text{M}-\text{C}$ σ -bond, thus starting a catalytic cycle. The problem is that the same factors that favor the nucleophilic attack, i.e., the positive charge on the metal ion and the resulting higher stability of the σ -bonded derivative, also disfavor the protolytic cleavage of the $\text{M}-\text{C}$ σ -bond.^{8–10} In practice, catalytic processes involving nitrogen nucleophiles have recently been achieved using amides rather than amines,¹¹ so that the poorly coordinating and poorly basic nucleophile does not compete with the olefin for coordination to the metal and at the same time produces a very acidic proton after the nucleophilic attack. Less well-balanced conditions would either produce no reaction at all or give a stable σ -bonded alkyl derivative that would not evolve further.^{4,5}

Another class of nucleophiles that could in principle react via a π -bonding pair are the aromatic rings, in a reaction quite similar to Friedel–Crafts alkylations. In this case, the reconstitution of the aromaticity from the primary intermediate would

* Corresponding author. E-mail: alvitagl@unina.it.

(1) Crabtree, R. H. *The Organometallic Chemistry of Transition Metals*, 4th ed.; John Wiley & Sons: New York, 2005.

(2) (a) Maresca, L.; Natile, G.; Rizzardi, G. *Inorg. Chim. Acta* **1980**, 38, 53. (b) Maresca, L.; Natile, G. *J. Chem. Soc., Chem. Commun.* **1983**, 40. (c) Maresca, L.; Natile, G. *Comments Inorg. Chem.* **1994**, 16, 95, and references therein.

(3) (a) Sasaki, S.; Maruta, K.; Ohkubo, K. *Inorg. Chem.* **1987**, 26, 2499. (b) Strömberg, S.; Svensson, M.; Zetterberg, K. *Organometallics* **1997**, 16, 3165.

(4) Hahn, C.; Morvillo, P.; Vitagliano, A. *Eur. J. Inorg. Chem.* **2001**, 419.

(5) Hahn, C.; Morvillo, P.; Herdtweck, E.; Vitagliano, A. *Organometallics* **2002**, 21, 1807.

(6) Haszeldine, R. N.; Parish, R. V.; Robbins, D. W. *J. Chem. Soc., Dalton Trans.* **1976**, 2355.

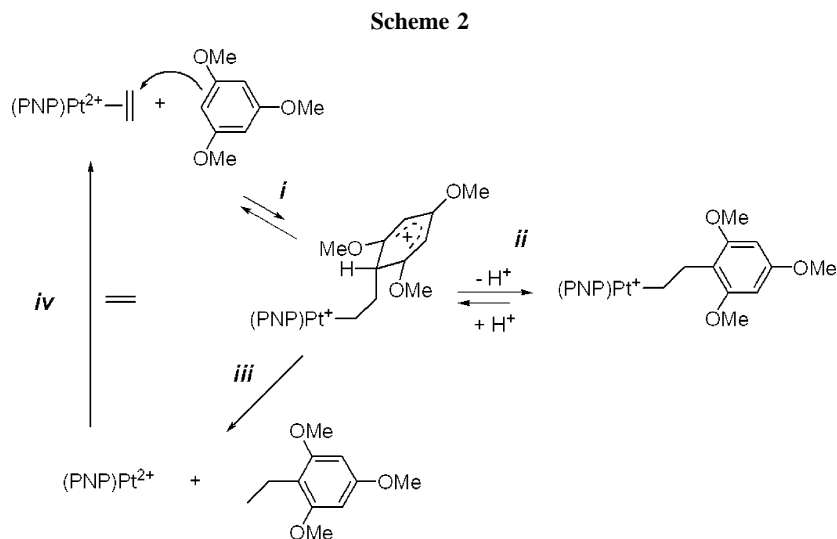
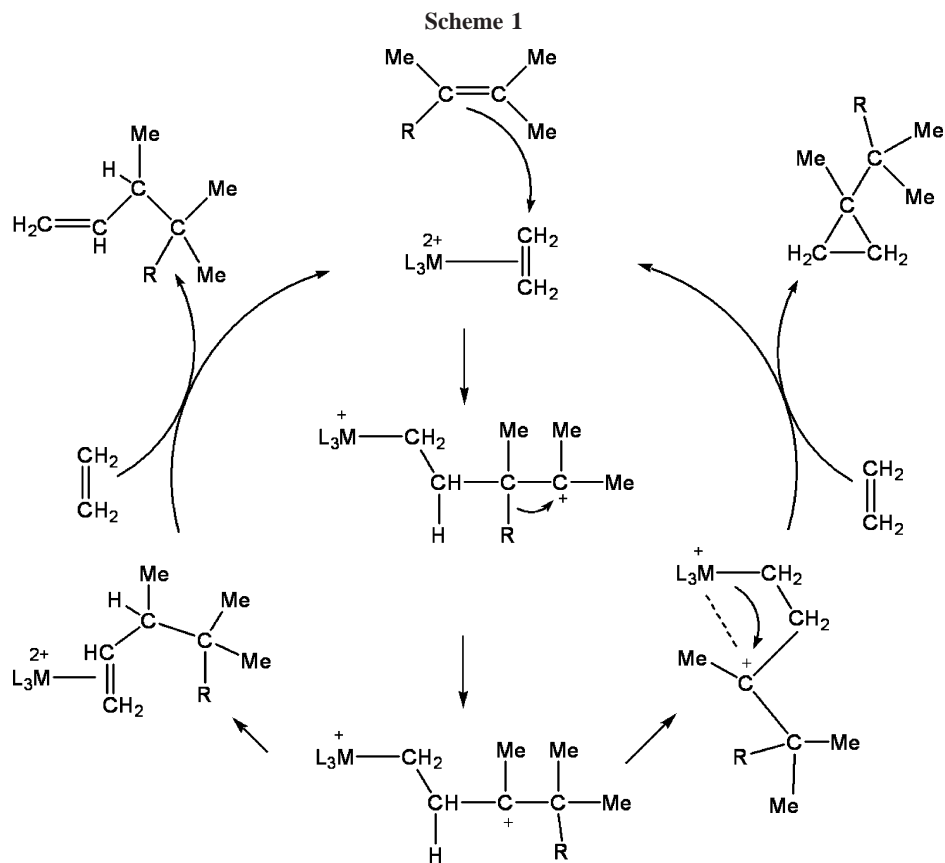
(7) (a) Hahn, C.; Cucciolito, M. E.; Vitagliano, A. *J. Am. Chem. Soc.* **2002**, 124, 9038. (b) Cucciolito, M. E.; D'Amora, A.; Vitagliano, A. *Organometallics* **2005**, 24, 3359.

(8) Whether the protonolysis takes place via a concerted three-center mechanism or via a prior oxidative addition to the metal,⁹ an interaction of the proton with the metal is involved, which is expected to be disfavored by the positive charge on the metal when the complex is cationic. Indeed, while in zwitterionic or neutral alkyl derivatives derived from the nucleophilic attack of amines on platinum-olefin complexes the $\text{M}-\text{C}$ bond is easily cleaved by HCl ,¹⁰ reversal of the attack was observed in cationic derivatives.⁵

(9) Romeo, R.; D'Amico, G. *Organometallics* **2006**, 25, 3435.

(10) Panunzi, A.; De Renzi, A.; Palumbo, R.; Paiaro, G. *J. Am. Chem. Soc.* **1969**, 91, 3879.

(11) (a) Karstedt, D.; Bell, A. T.; Tilley, T. D. *J. Am. Chem. Soc.* **2005**, 127, 12640. (b) Wang, X.; Widenhoefer, R. A. *Organometallics* **2004**, 23, 1649. (c) Bender, C. F.; Widenhoefer, R. A. *J. Am. Chem. Soc.* **2005**, 127, 1070. (d) Michael, F. E.; Cochran, B. M. *J. Am. Chem. Soc.* **2006**, 128, 4246.



release a proton, acidic enough to cleave the M–C σ -bond, thereby starting a catalytic cycle. Indeed, a Friedel–Crafts coupling of olefins with aromatic rings has been recently obtained in moderate yields using the combination of Zeise’s dimer and silver fluoroborate as catalyst,¹² but neither the truly active species nor any intermediate has been isolated. Following our previous studies⁷ on catalytic cross-coupling reactions promoted by highly electrophilic Pt²⁺ and Pd²⁺ species, we report in this paper an investigation of the stoichiometric and catalytic coupling of ethene and propene with arenes activated by methoxy substituents, including the X-ray characterization of a σ -bonded intermediate. The choice of methoxy substituents was suggested by the need to avoid activating substituents, such

as hydroxy or amino groups, which could themselves be good nucleophiles for the coordinated olefin.

Results and Discussion

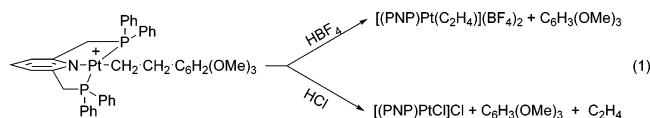
Reactions of the Ethene Complex [Pt(PNP)(C₂H₄)](SbF₆)₂ (1a) with 1,3,5-Trimethoxybenzene. In a preliminary test, the complex was reacted with a slight excess of 1,3,5-trimethoxybenzene in 9:1 CD₂Cl₂/CD₃NO₂ solution, and the reaction was monitored by ¹H NMR. Immediately after dissolution of the reactants, multiplets of very small intensity (accounting for less than 1% of the reactants) appeared at $\delta = 2.0$ and $\delta = 2.45$, indicating the presence of a Pt–CH₂–CH₂–Ar fragment. These signals did not grow further with time, but other signals appeared and slowly increased, which could be ascribed to the alkylation

(12) Karshedt, D.; Bell, A. T.; Tilley, T. D. *Organometallics* **2004**, *23*, 4169.

product 2-ethyl-1,3,5-trimethoxybenzene (**2**). After 4 h, 20% conversion of the substrate to the alkylation product was observed.

The spontaneous cleavage of the Pt–C σ -bond by the proton released from the aromatic ring indicated that the reaction can in principle be catalytic. Accordingly, we ran it in the presence of 30 equiv of 1,3,5-trimethoxybenzene under 1 bar pressure of ethene, and a very modest catalytic activity was in fact revealed, 2 equiv (with respect to the catalyst) of the alkylation product being obtained after 72 h at room temperature. The activity increased by switching to pure nitromethane as solvent (4 equiv after 72 h) and by raising the temperature (7 equiv being obtained in MeNO₂ after 24 h at 70 °C and 7 bar).

In another experiment, the addition of 20 μ L of water to the sample after the dissolution of the reactants caused the immediate formation of the σ -alkyl derivative [(PNP)PtCH₂CH₂–C₆H₂(OMe)₃][SbF₆ (**2a**), which in a larger scale experiment was isolated as fluoroborate salt and characterized by X-ray structural analysis (see later). In two different attempts to cleave the Pt–C σ -bond by addition of a strong acid, complex **2a** was treated with gaseous HCl and with HBF₄·Et₂O in dichloromethane solution. Somehow unexpectedly, in both cases no cleavage of the Pt–C σ -bond was observed, but the coupling reaction was reversed (eq 1), giving trimethoxybenzene and the complexes [Pt(PNP)Cl]Cl and [Pt(PNP)(C₂H₄)](BF₄)₂, respectively, in the former and latter case.



The above experiments indicate that the whole catalytic process proceeds through the mechanism depicted in Scheme 2. In a first rapid equilibrium step (*i*), the electrophilic-coordinated ethene molecule attacks the activated aromatic ring, forming a transient arenium ion as usual for Friedel–Crafts alkylations. Although fast (as proven by the immediate formation of the σ -alkyl species **2a**), this equilibrium is largely shifted toward the reactants, and only an extremely small amount of the arenium ion is probably present in solution. Indeed, the signals of the σ -bonded species revealed after mixing of the reagents coincide with those of the isolated complex **2a** and, therefore, most likely belong not to a true arenium ion but to its deprotonation product by traces of water present in the solvent mixture. The fast “side step” *ii* must also be reversible, as proven by the reversal of the coupling reaction after addition of a strong acid, while the “productive” step *iii*, involving the protolytic cleavage of the Pt–C σ -bond, is irreversible but very slow. The protonolysis of the Pt–C σ -bond leaves a coordination site available to a new ethene molecule, and the catalytic cycle is thus closed in step *iv*. The slowness of step *iii* is not surprising, since the protonolysis of the Pt–C σ -bond is expected to have a barrier increasing with the positive charge on the metal,⁸ but an open question is whether it is effected intramolecularly by the proton released by the arenium ion or intermolecularly by a proton first transferred to a water molecule present in the solvent or to the solvent itself. It is worth noting that isotope labeling experiments do not help in answering this question, because in the reaction mixture the protons on the activated aromatic ring are exchanging anyhow with protic species (e.g., water) present in the acidic medium. Nevertheless we tend to favor the hypothesis of the intramolecular cleavage, on the grounds that the addition of a strong acid failed to cleave the Pt–C σ -bond, causing instead the reversal of the ethene attack on the aromatic ring (eq 1).

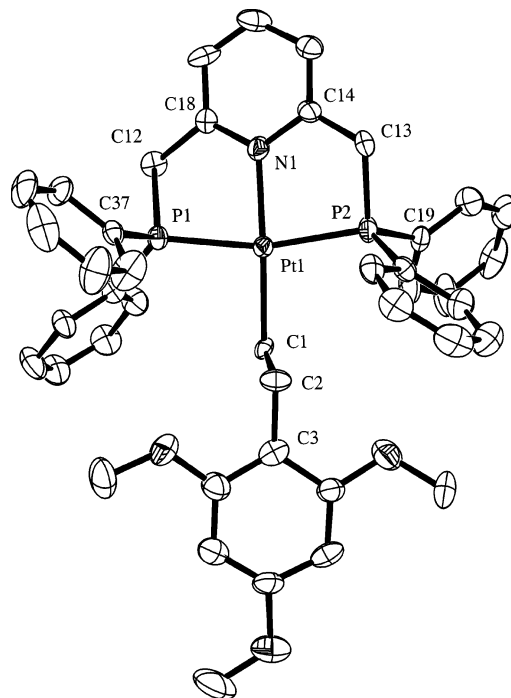


Figure 1. ORTEP drawing of the cation of complex **2a**. H atoms are not shown, and thermal ellipsoids are drawn at the 30% probability level.

Table 1. Selected Bond Lengths (Å), Bond Angles (deg), and Torsion Angles (deg) for **2a**–BF₄ with esd's in Parentheses

Pt1–P1	2.263(3)
Pt1–P2	2.282(3)
Pt1–N1	2.098(9)
Pt1–C1	2.157(9)
P1–C12	1.798(9)
P2–C13	1.844(11)
C1–C2	1.421(16)
C2–C3	1.520(17)
P1–Pt1–P2	164.9(1)
P1–Pt1–P2	82.2(3)
P1–Pt1–C1	95.5(3)
P2–Pt1–N1	83.9(3)
P2–Pt1–C1	98.7(3)
N1–Pt1–C1	176.6(4)
Pt1–C1–C2	116.3(7)
C1–C2–C3	109.7(9)
Pt1–C1–C2–C3	179.2(8)
P1–C12–C18–N1	25.7(13)
P2–C13–C14–N1	24.7(15)
C1–C2–C3–C4	94.2(15)

Molecular Structure of [(PNP)PtCH₂CH₂–C₆H₂(OMe)₃]-BF₄ (2a**–BF₄).** Single crystals of the compound suitable for X-ray analysis were obtained from a methylene chloride/diethyl ether solution. The molecular structure of the cation is shown in Figure 1, and selected bond lengths and angles are given in Table 1. The compound (monoclinic, space group *P2*₁/*c*) crystallizes with one square-planar cationic Pt complex and one separate BF₄[–] anion in the asymmetric unit. The PNP ligand acts as tridentate, exhibiting a local C₂ symmetry around the axis passing through the Pt–N bond, and the trimethoxyphenylethyl group is σ -bonded to the metal. The expected square-planar coordination geometry around the Pt atom is slightly distorted, owing to the constraints of the PNP chelate (bite angles N–Pt–P are 82.2(3)° and 83.9(3)°, P–N–P angle is 164.9(1)°). The Pt–C1 bond distance (2.157(9) Å) is slightly longer

Table 2. Yield and Product Distribution in the Reaction of Ethene with 1,3-Dimethoxybenzene under Various Conditions^a

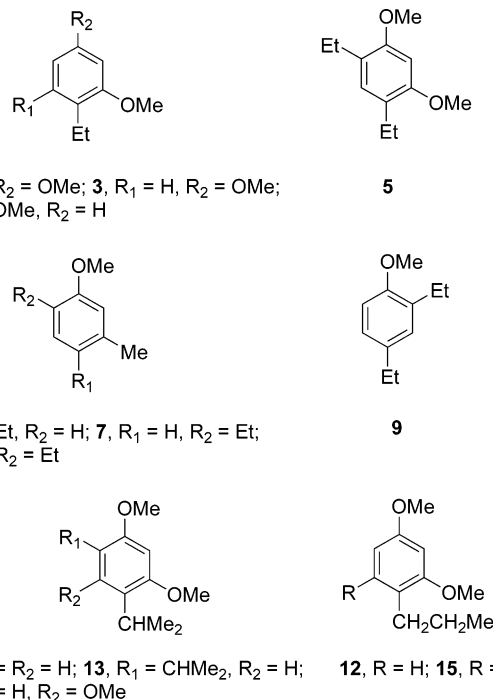
entry	no. equiv substrate	T (°C)	p (bar)	% reacted substrate	product distribution (mol %) ^b		
					3	4	5
1 ^c	30	24	1	16	86	14	0 ^d
2	30	24	1	50	57	15	28
3	30	24	7	83	40	21	39
4	30	70	7	100	35	0	65
5	50	70	7	100	31	8	61
6	75	70	7	80	68	13	19

^a Concentration of the catalyst (**1a**) before addition of the substrate: 0.10 M in nitromethane. ^bThe given abundances are relative to the major products. Other minor products cumulatively did not exceed 5% of the total. ^cSolvent: CH₂Cl₂ containing 10% MeNO₂. ^dDetectable in traces (<0.4%).

than expected for a Pt–C bond *trans* to nitrogen,¹³ and conversely, the Pt–N bond distance (2.098(9) Å) is slightly shorter than expected for a Pt–N bond *trans* to carbon.¹³ This may be due to the rigidity of the coordinated PNP and to its rather invariable structural features when changing the metal or the other ligand.^{5,14} The CH₂–CH₂ chain derived from the attack to the coordinated ethene molecule is in a *trans* conformation, as apparent from the value of the torsion angle Pt–C1–C2–C3 = 179.2(8)°. The trimethoxyphenyl group is all planar and roughly parallel to the coordination plane (angle between mean planes is 17.1(1)°), being stabilized in this conformation by a face-to-face van der Waals interaction with the pyridine ring of an adjacent molecule (distance between centroids is 3.825(3) Å).

Reactions of [Pt(PNP)(C₂H₄)](SbF₆)₂ (1a**) with 1,3-Dimethoxybenzene.** Although the disubstituted benzene ring of 1,3-dimethoxybenzene is in principle less activated than that of 1,3,5-trimethoxybenzene, the former proved to be more reactive in the coupling reaction. We tested the reaction under various catalytic conditions, and the results are reported in Table 2, the alkylation products being listed in Chart 1.

As in the case of 1,3,5-trimethoxybenzene, the addition of 20 μL of water to a NMR sample of **1a** and 1,3-dimethoxybenzene in 9:1 CD₂Cl₂/CD₃NO₂ caused the immediate conversion of the complex to a mixture of the *σ*-alkyl derivatives **3a**–**5a** (Chart 2).¹⁵ The slow formation of the cleavage products **3**–**5** under catalytic conditions, compared to the rapid formation of **3a**–**5a** under the assistance of a base (H₂O), suggested the addition step to be fast and reversible¹⁶ and the Pt–C bond

Chart 1. Alkylated Arenes Resulting from the Cross-Coupling Reactions

cleavage to be the rate-determining step of the catalytic reaction as in the case of 1,3,5-trimethoxybenzene reported above. However, the reaction of the *σ*-alkyl derivatives **3a**–**5a** with gaseous HCl in CH₂Cl₂ solution gave the corresponding alkylated arenes **3**–**5**, while in the case of **2a** only the reversal of the coupling reaction (eq 1) was observed. The different behavior may be explained by the higher stability of the transient arenium ion for **2a** compared to **3a**–**5a**, which directs the proton attack on the aromatic ring rather than on the Pt–C *σ*-bond. This also explains the lower reactivity of 1,3,5-trimethoxybenzene in the catalytic reaction, since the higher stability of the arenium ion is expected to slow down the rate-determining Pt–C *σ*-bond cleavage.

Reactivity of [Pt(PNP)(C₂H₄)](SbF₆)₂ (1a**) with Other Substrates.** Moving to a less activated aromatic ring, we treated **1a** in MeNO₂ solution with a 10-fold molar excess of 3-methylanisole under 1 atm pressure of ethene at room temperature. A sluggish reaction was observed, and 2 equiv of a mixture of the alkylation products **6** and **7** was formed after 96 h at room temperature. However by performing the reaction at 70 °C with 30 and 50 equiv of 3-methylanisole under a 7 bar pressure of ethene, a complete conversion of the substrate to the dialkylated product **8** was surprisingly obtained (Table 3, entries 1 and 2), with only tiny amounts of the monoalkylated products **6** and **7**. However, when we performed the base-assisted stoichiometric reaction by adding 20 μL of water to a NMR sample of **1a** and 3-methylanisole (2 equiv) in CD₃NO₂, the corresponding *σ*-alkyl derivatives **6a** and **7a** were not formed immediately, but with an approximate half-life of the starting complex of 50 min, a complete conversion being observed in ca. 3 h. As expected, treating the mixture of the *σ*-alkyl derivatives **6a** and **7a** with gaseous HCl in CH₂Cl₂ caused the immediate cleavage of the Pt–C *σ*-bond, giving the corresponding alkylated arenes **6** and **7**.

The effect of further decreasing the aromatic ring activation was probed by using anisole. In this case no reaction was obtained at room temperature, and even the base-assisted addition was sluggish and did not produce clean *σ*-alkyl

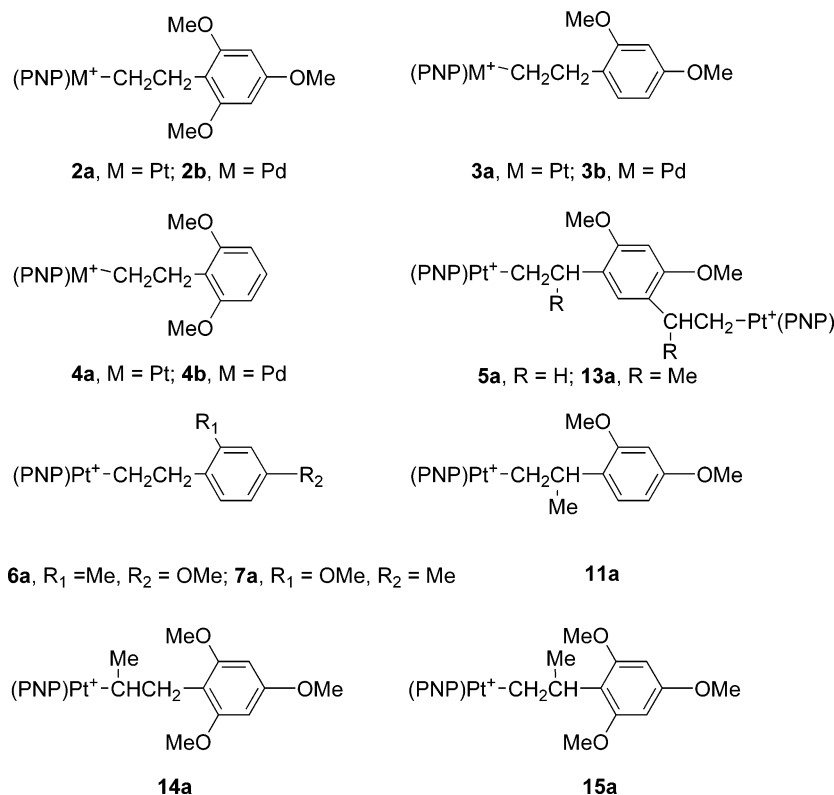
(13) (a) Zhao, S.-B.; Wu, G.; Wang, S. *Organometallics* **2006**, *25*, 5979. (b) Wile, B. M.; Burford, R. J.; McDonald, R.; Ferguson, M. J.; Stradiotto, M. *Organometallics* **2006**, *25*, 1028. (c) Ganis, P.; Orabona, I.; Ruffo, F.; Vitagliano, A. *Organometallics* **1998**, *17*, 2646.

(14) (a) Hahn, C.; Vitagliano, A.; Giordano, F.; Taube, R. *Organometallics* **1998**, *17*, 2060. (b) Steffey, B. D.; Miedaner, A.; Maciejewski-Farmer, M. L.; Bernatis, P. R.; Herring, A. M.; Allured, V. S.; Carperos, V.; DuBois, D. L. *Organometallics* **1994**, *13*, 4844. (c) Barloy, L.; Ramdeehul, S.; Osborn, J. A.; Carlotti, C.; Taulelle, F.; De Cian, A.; Fischer, J. *Eur. J. Inorg. Chem.* **2000**, 2523. (d) Hahn, C.; Sieler, J.; Taube, R. *Chem. Ber.* **1997**, *130*, 393.

(15) To help their identification by ¹H and ¹³C NMR, **3a**–**5a** were isolated (without separation) from two larger scale reactions, run in the presence of different amounts of the aromatic substrate. Using a slight excess of 1,3-dimethoxybenzene **3a**, **4a**, and **5a** were obtained in 47%, 15%, and 38% molar abundances, respectively. A 10-fold excess of the aromatic substrate favored the monosubstituted products, yielding **3a**, **4a**, and **5a** in 85%, 10%, and 5% molar abundances, respectively.

(16) The reversibility of the addition step was proven by dissolving a mixture of **3a**, **4a**, and **5a** (47%, 15%, and 38%, respectively) in CD₂Cl₂, in the presence of 4 equiv of 1,3-dimethoxybenzene and 0.5 equiv of etherated HBF₄. The solution equilibrated within a few minutes, giving a mixture of 90% **3a**, 10% **4a**, and only traces of **5a**.

Chart 2. Alkyl Derivatives Resulting from the Base-Assisted Stoichiometric Reactions

Table 3. Yield and Product Distribution in the Reactions of Ethene and Propene with Different Substrates^a

entry	catalyst, olefin	substrate, ^b no. equiv	% reacted substrate	relative products distribution ^c (mol %)		
1	1a , ethene	man , 30	100	8 , 100		
2	1a , ethene	man , 50	100	8 , 100		
3	1a , ethene	an , 30	100	9 , 100		
4	1a , ethene	an , 50	100	9 , 100		
5	10a , propene ^d	dmb , 30	40	11 , 70	12 , 15	13 , 15
6	1b , ethene	dmb , 30	35	3 , 85	4 , 10	5 , 5

^a Solvent: nitromethane; $T = 70\text{ }^{\circ}\text{C}$; $p = 7\text{ bar}$. ^b **dmb** = 1,3-dimethoxybenzene; **man** = 3-methylanisole; **an** = anisole. ^c The given abundances are relative to the three major products. Other minor products cumulatively did not exceed 5% of the total. ^d $p = 2\text{ bar}$.

derivatives. By contrast, running the reaction at $70\text{ }^{\circ}\text{C}$ under a 7 bar pressure of ethene, a complete conversion of the substrate was observed, leading almost exclusively to the dialkylated product **9** (Table 3, entries 3 and 4).

The above results show that, by reducing the activation of the aromatic ring, the rate of the addition step is correspondingly reduced (and so is the equilibrium constant for the formation of the arenium ion), while the rate of the Pt–C σ -bond cleavage is increased due to the increased acidity of the arenium ion. In the case of 3-methylanisole and anisole the rates of the two steps are probably comparable and a productivity even larger than in the case of 1,3-dimethoxybenzene was observed when running the catalytic reaction at $70\text{ }^{\circ}\text{C}$, as shown by the complete conversion of the substrate to the dialkylated product (entries 2 and 4 in Table 3 versus entry 5 in Table 2).

Reactivity of [Pt(PNP)(CH₂=CHMe)](SbF₆)₂ (10a**).** Propene proved to be less reactive than ethene in the catalytic coupling reactions. At room temperature and using a moderate excess of substrate, no reaction was observed with 1,3,5-trimethoxybenzene and a very sluggish reaction took place with 1,3-dimethoxybenzene (less than 1 equiv reacted after 4 days).

At $70\text{ }^{\circ}\text{C}$ and using a larger excess (30 equiv) of 1,3-dimethoxybenzene under a 2 bar pressure of propene, a 40% conversion of the substrate to a mixture of the alkylated products **11**, **12**, and **13** (in 70%, 15% and 15% molar abundances, see Table 3, entry 5) was observed. Quite interesting was the result of the base-assisted reactions with 1,3,5-trimethoxybenzene and 1,3-dimethoxybenzene, which were performed by adding 2.5 equiv of the aromatic substrate, 5 equiv of propene, and 10 μL of water to a solution of **10a** in CD_3NO_2 and monitored by ¹H NMR. In contrast to the case of the ethene complex **1a**, the reactions were not immediate. The reaction with 1,3,5-trimethoxybenzene took place with an approximate half-life of 10 min, but reached an equilibrium within 30 min, giving a mixture of 40% starting complex **10a**, 35% **14a** (anti-Markovnikov addition product), and 25% **15a** (Markovnikov addition product). The equilibrium was completely shifted to the σ -alkyl products by further addition of water. The reaction with 1,3-dimethoxybenzene took place much more slowly, with an approximate half-life of 3 h, but finally producing a 90:10 mixture of the Markovnikov products **11a** and **13a**, with a tiny amount of the anti-Markovnikov monoalkylated product and no detectable amount of the starting complex left at equilibrium.

The above results clarify some further details of the general picture given in Scheme 2. If we just consider the stoichiometric addition to give the σ -alkyl complex, this consists of the rate-determining formation of an arenium ion (step *i* in Scheme 2), followed by a fast proton transfer (step *ii* in Scheme 2) from the arenium ion to an external base (H_2O in our case). Both are equilibrium reactions, and the overall equilibrium constant K is given by $K = K_i K_{ii}$, while the overall reaction rate is determined by the forward kinetic constant k_i of the first step. The rate of the first step appears to be controlled by the stability of the arenium ion, with the rate constant k_i and the equilibrium constant K_i increasing with the number of electron-releasing methoxy substituents. The equilibrium constant K_{ii} of the proton-

transfer step is also controlled by the stability of the arenium ion, but in the reverse way, an increasing number of electron-releasing methoxy substituents *decreasing* the acidity of the arenium ion and thus disfavoring the proton transfer. The above experiments show that upon going from 1,3-dimethoxybenzene to 1,3,5-trimethoxybenzene, while the kinetic constant increases, the overall equilibrium constant K *decreases*, which can quite reasonably be ascribed to the steric hindrance of the carbon chain placed between two *ortho* substituents in **14a** and **15a**. This steric hindrance also accounts for the 60% anti-Markovnikov addition in the case of 1,3,5-trimethoxybenzene versus more than 95% Markovnikov addition in the case of 1,3-dimethoxybenzene (**11a** and **13a**).

About the catalytic coupling reaction, it is interesting to note that the amount of the anti-Markovnikov product **12** produced was substantially larger than that observed in the stoichiometric addition. Most likely, the σ -alkylarenium ion containing a branched alkyl chain bound to the metal is less stable and so it does give a small amount of product in the stoichiometric reaction, but for the very same reason it is more reactive to the protolytic cleavage, resulting in the observed product distribution (Table 3, entry 5). The lower reactivity of propene compared to ethene can be ascribed to a lower concentration of the arenium ion (under similar conditions), due to a lower value of the addition equilibrium constant K_i . This is consistent with the results obtained in the case of the nucleophilic attack of amines, where the addition constant was found to be 1–2 orders of magnitude smaller for propene than for ethene.^{4,5} To directly confirm this hypothesis, we did a competitive experiment, in which a NMR sample containing equimolar amounts (10 μ mol) of the ethene complex **1a** and of the propene complex **10a** in the presence of a slight excess of 1,3,5-trimethoxybenzene in CD_3NO_2 was treated with 3 μ L of water. Under these conditions 75% of the ethene complex was converted to the σ -alkyl derivative **2a**, while less than 1% of the propene complex gave the corresponding species **14a** and **15a**, indicating that the addition to the propene complex is indeed thermodynamically less favored by at least 2 orders of magnitude of K_i .

Reactivity of [Pd(PNP)(C₂H₄)](SbF₆)₂ (1b**).** The palladium complex proved to be less reactive in the catalytic reaction compared to its platinum analogue **1a**. At room temperature, no reaction at all was observed with 1,3,5-trimethoxybenzene and only traces of the coupling product **3** were observed with 1,3-dimethoxybenzene after 48 h. A modest activity was observed at 70 °C, where a 35% conversion to a mixture of **3**, **4**, and **5** (85%, 10%, and 5% molar abundances, respectively) was observed in 24 h using 30 equiv of 1,3-dimethoxybenzene under a 7 bar pressure of ethene (Table 3, entry 6). These results suggest that also in the palladium case the protolytic cleavage of the M–C σ -bond is the rate-determining step of the catalytic reaction, as discussed in the case of the platinum complex. Indeed, the base-assisted addition of both 1,3,5-trimethoxybenzene and 1,3-dimethoxybenzene, performed as described for the platinum complex **1a**, within a couple of minutes gave the σ -alkyl derivatives **2b** and **3b–4b**, respectively. To assess whether the lower catalytic activity of the palladium complex compared to the platinum complex is due to a lower value of the addition equilibrium constant K_i or to a higher barrier to the protolytic cleavage, we did a competitive experiment similar to the one described above. A NMR sample containing equimolar amounts (10 μ mol) of the platinum complex **1a** and of the palladium complex **1b** in the presence of a slight excess of 1,3,5-trimethoxybenzene in CD_3NO_2 was treated with 4 μ L of water. The solution equilibrated within a few minutes, and

the relative abundances of the four species at equilibrium (**1a**, **1b**, **2a**, **2b**) were determined by integration of appropriate signals in the equilibrium mixture, leading to an estimate for the ratio of the addition constants $K_{i(\text{Pt})}/K_{i(\text{Pd})}$ of about 8. Since this value appears to be not large enough to be the only source of the markedly larger reactivity of the platinum species in the catalytic reactions, it can be inferred that also the rate constant of the protolytic cleavage is higher for the platinum σ -alkyl complexes than for the corresponding palladium species. This is not surprising, if a protonolysis mechanism is considered in which the proton either oxidatively adds to the metal or simultaneously interacts with the metal and the carbon atoms in a three-center transition state.⁸ In both cases either a full or a partial oxidative addition to the metal is involved, which is expected to be easier for platinum than for palladium.

Conclusions

The results reported in this paper show that the coordination to dicationic Pt^{2+} and Pd^{2+} species enhances the electrophilicity of an olefin to the point of promoting the attack to aromatic rings activated by electron-donating substituents such as methoxy groups. The reaction can take place catalytically, since the proton released by the intermediate arenium ion is able to cleave the M–C σ -bond. The consistent qualitative picture emerging from the results shows the influence of the ring substituents on the rates of the two crucial steps of the catalytic reaction, i.e., the attack of the coordinated olefin to the aromatic ring (step *i* in Scheme 2) and the successive (most likely intramolecular) protolytic cleavage of the M–C σ -bond (step *iii* in Scheme 2). Decreasing the activation of the aromatic ring decreases the rate of the attack but increases the rate of the protolytic cleavage, so that in the delicate interplay between the two effects an aromatic ring that is less activated to the stoichiometric coupling can become more reactive in the catalytic reaction, as is the case of anisole and 3-methylanisole versus 1,3-dimethoxybenzene and 1,3,5-trimethoxybenzene. Looking at the influence of the olefin and the metal, it also appears that changing the olefin from ethene to propene considerably disfavors the attack, without having much effect on the rate of the protolytic cleavage, while switching from Pt^{2+} to Pd^{2+} disfavors the attack, but also slows the rate of the protolytic cleavage.

As a final remark, we note that apart from the potential synthetic uses of the reaction, a major conceptual interest lies in a catalytic process in which the single steps can be performed at a stoichiometric level and the trends controlling them can be satisfactorily rationalized.

Experimental Section

General Procedures. CD_2Cl_2 , CD_3NO_2 , and MeNO_2 (free from nitriles) were dried with 4 Å molecular sieves. The aryl substrates were obtained by Aldrich and were used without further purification. The NMR spectra were recorded on Varian VXR 200, Varian Gemini 300, and Bruker WH 400 instruments. The ¹H NMR shifts were referenced to the resonance of the residual protons of the solvents; the ¹³C NMR shifts, to the solvent resonance ($\delta = 53.8$, CD_2Cl_2 ; $\delta = 62.8$, CD_3NO_2). Abbreviations used in NMR data: s, singlet; d, doublet; t, triplet; ps t, pseudo triplet; m, multiplet; br, broad.

Syntheses. The complexes $[\text{Pt}(\text{PNP})(\text{CH}_2=\text{CHR})](\text{SbF}_6)_2$ and $[\text{Pd}(\text{PNP})(\text{CH}_2=\text{CH}_2)](\text{SbF}_6)_2$ were prepared according to the procedures described in the literature.^{4,5}

Preparation of σ -Derivatives. General Procedure. To a solution of the alkene complex (0.04 mmol) in 2 mL of CH_2Cl_2 were added 1.5 equiv of aryl compound and 20 μ L of H_2O . The

mixture was stirred for 15 min (2 h in the case of 3-methylanisole and 4 h in the case of the propene complex with all the aryl derivatives). The solution was dried over Na_2SO_4 , filtered, and concentrated *in vacuo*. The product was precipitated by dropwise addition of diethyl ether, filtered off, and dried under vacuum. Except for the case of 1,3,5-trimethoxybenzene a mixture of alkyl derivatives was obtained. Since initial separation attempts were unsuccessful, the complexes were characterized directly in their mixture by ^1H and ^{13}C NMR. In addition, the assigned structures were confirmed by reductive and/or protolytic degradation of the complex mixture and successive identification of the resulting organic products.

2a. Yield: 97%; whitish solid. Anal. Calcd for $\text{C}_{42}\text{H}_{42}\text{F}_6\text{NO}_3\text{P}_2\text{-PtSb}$: C, 45.80; H, 3.84; N, 1.27. Found: C, 45.73; H 3.89; N, 1.26. ^1H NMR (300 MHz, CD_2Cl_2): δ 2.02 (m, 2 H, PtCH_2 , $J_{\text{Pt}} = 78$ Hz), 2.45 (m, 2 H, CH_2Ar), 3.36 (s, 6 H, OMe), 3.67 (s, 3 H, OMe), 4.37 (ps t, 4 H, PCH_2), 5.93 (s, 2 H, Ar), 7.50–7.90 (m, 22 H, PPh, py), 8.02 (t, 1 H, py). ^{13}C NMR (75 MHz, CD_2Cl_2): δ 1.1 ($J_{\text{Pt}} = 585$ Hz, PtCH_2), 27.9 (CH_2Ar), 46.9 (ps t, $J_{\text{P}} = 30$ Hz, PCH_2), 55.5 (OMe), 90.7 (C-3 and C-5, Ar), 114.7 (C-1, Ar), 123.0 (py-3,5), 128.0 (ps t, $J_{\text{P}} = 54$ Hz, PPh_j), 130.0 (PPh_m), 132.5 (PPh_p), 133.5 (PPh_o), 140.2 (py-4), 158.3 (C-2 and C-6, Ar), 159.2 (C-4, Ar), 159.7 (ps t, $J_{\text{Pt}} = 35$ Hz, py-2,6).

2b. Yield: 94%; white solid. Anal. Calcd for $\text{C}_{42}\text{H}_{42}\text{F}_6\text{NO}_3\text{P}_2\text{-PdSb}$: C, 49.81; H, 4.18; N, 1.38. Found: C, 49.75; H, 4.27; N, 1.36. ^1H NMR (300 MHz, CD_2Cl_2): δ 2.14 (m, 2 H, PdCH_2), 2.64 (m, 2 H, CH_2Ar), 3.40 (s, 6 H, OMe), 3.70 (s, 3 H, OMe), 4.36 (ps t, 4 H, PCH_2), 5.96 (s, 2 H, Ar), 7.40–7.80 (m, 22 H, PPh, py), 7.93 (ps t, 1 H, py). ^{13}C NMR (75 MHz, CD_2Cl_2): δ 17.2 (PdCH_2), 26.9 (CH_2Ar), 45.5 (ps t, $J_{\text{P}} = 26$ Hz, PCH_2), 55.6 (OMe), 90.7 (C-3 and C-5, Ar), 112.8 (C-1, Ar), 123.0 (py-3,5), 128.9 (ps t, $J_{\text{P}} = 45$ Hz, PPh_j), 130.0 (PPh_m), 132.1 (PPh_p), 133.3 (ps t, PPh_o), 140.8 (py-4), 158.3 (C-2, C-4, and C-6, Ar), 159.4 (py-2,6).

3a (in a mixture with **4a** and **5a**). ^1H NMR (300 MHz, CD_2Cl_2): δ 1.98 (m, 2 H, PtCH_2), 2.34 (m, 2 H, CH_2Ar), 3.41 (s, 3 H, OMe), 3.73 (s, 3 H, OMe), 4.40 (m, PCH_2), 6.16 (dd, 1 H, Ar), 6.22 (s, 1 H, Ar), 6.24 (d, 1 H, Ar), 7.44–8.06 (m, PPh, py). ^{13}C NMR (50 MHz, CD_2Cl_2): δ 2.4 (PtCH_2), 35.0 (CH_2Ar), 46.4 (ps t, $J_{\text{P}} = 35$ Hz, PCH_2), 55.5 (OMe), 98.3 (C-3, Ar), 104.2 (C-5, Ar), 123.0 (py-3,5), 127.0 (C-1, Ar), 127.8 (ps t, $J_{\text{P}} = 54$ Hz, PPh_j), 129.5 (C-6, Ar), 130.0 (PPh_m), 132.5 (PPh_p), 133.5 (PPh_o), 140.3 (py-4), 158.0 (C-2, Ar), 159.0 (C-4, Ar), 159.5 (ps t, $J_{\text{Pt}} = 38$ Hz, py-2,6).

4a (in a mixture with **3a** and **5a**). ^1H NMR (300 MHz, CD_2Cl_2): δ 2.18 (m, PtCH_2 overlapped by signals from **5a**), 2.52 (m, 2 H, CH_2Ar), 3.38 (s, 6 H, OMe), 4.40 (m, PCH_2), 6.34 (d, 2 H, Ar), 6.96 (t, 1 H, Ar), 7.44–8.06 (m, PPh, py).

5a (in a mixture with **3a** and **4a**). ^1H NMR (300 MHz, CD_2Cl_2): δ 1.86 (m, 4 H, PtCH_2), 2.18 (m, CH_2Ar), 3.36 (s, 6 H, OMe), 4.40 (m, PCH_2), 5.64 (s, 1 H, Ar), 6.06 (s, 1 H, Ar), 7.44–8.06 (m, PPh, py).

3b (in a mixture with **4b**) Yield: 94%; white solid. Anal. Calcd for $\text{C}_{41}\text{H}_{40}\text{F}_6\text{NO}_2\text{P}_2\text{-PdSb}$: C, 50.11; H 4.10; N, 1.43. Found: C, 49.89; H, 4.22; N, 1.41. ^1H NMR (300 MHz, CD_2Cl_2): δ 2.10 (m, 2 H, PdCH_2), 2.50 (m, 2 H, CH_2Ar), 3.45 (s, 3 H, OMe), 3.69 (s, 3 H, OMe), 4.41 (ps t, 4 H, PCH_2), 6.20 (dd, 1 H, Ar), 6.26 (d, 1 H, Ar), 6.33 (d, 1 H, Ar), 7.50–7.80 (m, PPh, py), 7.91 (t, 1 H, py). ^{13}C (75 MHz, CD_2Cl_2): δ 17.7 (PdCH_2), 33.5 (CH_2Ar), 45.0 (ps t, $J_{\text{P}} = 28$ Hz, PCH_2), 55.5 (OMe), 98.7 (C-3, Ar), 104.3 (C-5, Ar), 123.3 (py-3,5 PPh_j), 125.1 (C-1, Ar), 128.7 (ps t, $J_{\text{P}} = 43$ Hz, PPh_j), 129.4 (C-6, Ar), 130.0 (PPh_m), 132.0 (PPh_p), 133.4 (PPh_o), 140.9 (py-4), 158.0 (C-2, Ar), 158.3 (py-2,6), 159.4 (C-4, Ar).

4b (in a mixture with **3b**). ^1H NMR (300 MHz, CD_2Cl_2): δ 2.36 (m, 2 H, PdCH_2), 2.71 (m, 2 H, CH_2Ar), 3.41 (s, 6 H, OMe), 4.38 (ps t, 4 H, PCH_2), 6.37 (d, 2 H, Ar), 6.99 (t, 1 H, Ar), 7.50–8.00 (m, PPh, py).

6a (in a mixture with **7a**). Yield: 95%; white solid. Anal. Calcd for $\text{C}_{41}\text{H}_{40}\text{F}_6\text{NOP}_2\text{-PtSb}$: C, 46.66; H, 3.82; N, 1.33. Found: C, 47.00; H, 3.67; N, 1.32. ^1H NMR (300 MHz, CD_2Cl_2): δ 1.54 (s, 3 H, Me–Ar), 1.90 (m, 2 H, PtCH_2), 2.34 (m, CH_2Ar), 3.62 (s, 3 H, OMe), 4.42 (ps t, 4 H, PCH_2), 6.26 (d, 1 H, Ar), 6.39 (dd, 1 H, Ar), 6.41 (d, 1 H, Ar), 7.50–7.90 (m, PPh, py), 8.00 (t, 1 H, py). ^{13}C NMR (75 MHz, CD_2Cl_2): δ 2.70 (PtCH_2 , $J_{\text{Pt}} = 637$ Hz), 19.0 (MeAr), 38.0 (CH_2Ar), 46.6 (ps t, $J_{\text{P}} = 31$ Hz, PCH_2), 55.4 (OMe), 111.1 (C-3, Ar), 115.6 (C-5, Ar), 123.1 (py-3,5), 127.3 (ps t, $J_{\text{P}} = 50$ Hz, PPh_j), 128.9 (C-1, Ar), 129.3 (C-6, Ar), 130.0 (PPh_m), 132.7 (PPh_p), 133.6 (PPh_o), 136.4 (C-2, Ar), 140.2 (py-4), 157.6 (C-4, Ar), 159.6 (ps t, $J_{\text{Pt}} = 33$ Hz, py-2,6).

7a (in a mixture with **6a**). ^1H NMR (300 MHz, CD_2Cl_2): δ 1.98 (m, 2 H, PtCH_2), 2.18 (s, 3 H, Me–Ar), 2.34 (m, CH_2Ar overlapped by signals from **6a**), 3.42 (s, 3 H, OMe), 4.40 (ps t, 4 H, PCH_2), 6.22 (d, 1 H, Ar), 6.44 (d, 1 H, Ar), 6.47 (s, 1 H, Ar), 7.50–7.90 (m, PPh, py), 8.02 (t, 1 H, py). ^{13}C NMR (75 MHz, CD_2Cl_2): δ 2.3 (PtCH_2), 21.4 (MeAr), 35.2 (CH_2Ar), 46.4 (ps t, $J_{\text{P}} = 35$ Hz, PCH_2), 55.2 (OMe), 111.6 (C-3, Ar), 121.0 (C-5, Ar), 123.1 (py-3,5), 127.7 (ps t, $J_{\text{P}} = 50$ Hz, PPh_j), 130.0 (PPh_m), 131.3 (C-6, Ar), 132.7 (PPh_p), 133.6 (PPh_o), 140.2 (py-4), 156.9 (C-2, Ar), 159.6 (py-2,6 overlapped by signals from **6a**).

11a (in a mixture with **13a**). ^1H NMR (300 MHz, CD_2Cl_2): δ 0.60 (d, 3 H, Me), 1.85 (m, 1 H, Pt– CHH , $J_{\text{Pt}} = 72$ Hz), 2.46 (m, 1 H, Pt– CHH , $J_{\text{Pt}} = 78$ Hz), 3.02 (m, 1 H, CH–Ar), 3.30 (s, 3 H, OMe), 3.68 (s, 3 H, OMe), 4.45 (m, 4 H, PCH_2), 6.19 (d, 1 H, Ar), 6.22 (s, 1 H, Ar), 6.53 (d, 1 H, Ar), 7.45–7.90 (m, PPh, py), 8.02 (t, 1 H, py). ^{13}C NMR (75 MHz, CD_2Cl_2): δ 11.6 ($J_{\text{Pt}} = 646$ Hz, PtCH_2), 24.7 (MeCH), 37.8 (CHMe), 46.8 (ps t, $J_{\text{P}} = 34$ Hz, PCH_2), 55.0 (OMe), 55.5 (OMe), 98.3 (C-3, Ar), 104.2 (C-5, Ar), 123.1 (py-3,5), 126.2 (C-6, Ar), 127.5 (ps t, $J_{\text{P}} = 57$ Hz, PPh_j), 128.5 (ps t, $J_{\text{P}} = 55$ Hz, PPh_j), 129.7 (PPh_m), 131.5 (C-1, Ar), 132.3 (PPh_p), 132.5 (PPh_p), 133.2 (PPh_o), 133.6 (PPh_o), 140.2 (py-4), 157.1 (C-2, Ar), 158.7 (C-4, Ar), 159.6 (ps t, $J_{\text{Pt}} = 35$ Hz, py-2,6).

13a (two diastereomers in equal abundance (in a mixture with **11a**)). ^1H NMR (300 MHz, CD_2Cl_2): δ 0.42 (d, Me), 0.48 (d, Me), 2.85 (m, CH), 3.21 (s, OMe), 3.34 (s, OMe), 5.99 (s, Ar), 6.01 (s, Ar), 6.02 (s, Ar), 6.03 (s, Ar), 7.45–7.90 (m, PPh, py).

14a (in a mixture with **15a**). Yield: 92%; white solid. Anal. Calcd for $\text{C}_{43}\text{H}_{44}\text{F}_6\text{NO}_3\text{P}_2\text{-PtSb}$: C, 46.30; H, 3.98; N, 1.26. Found: C, 46.26; H, 4.05; N, 1.25. ^1H NMR (300 MHz, CD_2Cl_2): δ 0.87 (d, 3 H, Me, $J_{\text{Pt}} = 53$ Hz), 2.27 (t, 1 H, CHH –Ar), 2.40 (m, 1 H, Pt–CH), 2.82 (dd, 1H, CHH –Ar), 3.30 (s, 6 H, OMe), 3.66 (s, 3 H, OMe), 4.20–4.55 (m, PCH_2), 5.88 (s, 2H, Ar), 7.45–8.05 (m, PPh, py). ^{13}C (50 MHz, CD_2Cl_2): δ 22.3 (PtCH), 24.5 (Me), 33.6 (CH_2Ar), 46.6 (ps t, $J_{\text{P}} = 36$ Hz, PCH_2), 55.3 (OMe), 90.4 (C-3 and C-5, Ar), 111.5 (C-1, Ar), 123.2 (py-3,5), 128.1 (ps t, $J_{\text{P}} = 53$ Hz, PPh_j), 129.7 (PPh_m), 132.6 (PPh_p), 133.2 (PPh_o), 140.3 (py-4), 158.8 (ps t, $J_{\text{Pt}} = 35$ Hz, py-2,6), 159.0 (C-2 and C-4, Ar), 159.7 (C-6, Ar).

15a (in mixture with **14a**). ^1H NMR (300 MHz, CD_2Cl_2): δ 0.72 (d, 3 H, Me), 2.42 (m, 1 H, Pt– CHH), 2.55 (m, 1 H, Pt– CHH), 3.17 (s, 6 H, OMe), 3.40 (m, 1 H, CH–Ar), 3.68 (s, 3 H, OMe), 4.20–4.55 (m, PCH_2), 5.89 (s, 2 H, Ar), 7.45–8.05 (m, PPh, py). ^{13}C NMR (50 MHz, CD_2Cl_2): δ 1.1 (PtCH_2), 13.4 (Me), 37.2 (CHAr), 47.0 (ps t, $J_{\text{P}} = 36$ Hz, PCH_2), 55.5 (OMe), 90.4 (C-3 and C-5, Ar), 111.5 (C-1, Ar), 123.2 (py-3,5), 127.6 (ps t, $J_{\text{P}} = 57$ Hz, PPh_j), 130.0 (PPh_m), 132.2 (PPh_p), 134.4 (PPh_o), 140.3 (py-4), 158.8 (ps t, $J_{\text{Pt}} = 35$ Hz, py-2,6), 159.0 (C-2 and C-4, Ar), 159.7 (C-6, Ar).

Catalytic Reactions. The catalytic reactions were run in a small glass autoclave under the conditions reported in Tables 2 and 3. The appropriate metal complex (0.03 mmol) was dissolved in 0.3 mL of anhydrous MeNO_2 (free from nitriles), and 20–75 equiv of the appropriate aryl compound was added (see Tables 2 and 3). The solution was stirred under ethene or propene for 24 h and then

evaporated to dryness, and the residue was extracted with diethyl ether. The solution was separated and evaporated to dryness, and the residue was analyzed by ^1H NMR.

Reductive Degradation with NaBH_4 . The reduction was performed on all the σ -alkyl derivatives. The mixture of complexes resulting from the base-assisted addition reaction (30–50 mg) was dissolved in 1.5 mL of $\text{CH}_2\text{Cl}_2/\text{MeOH}$ (5:2), and an excess of solid NaBH_4 was added. The mixture was stirred for 12 h and then treated with 1.0 mL of a NH_4Cl -saturated aqueous solution. The organic phase was separated and evaporated to dryness. The residue was extracted with diethyl ether, the ether extract was evaporated to dryness, and the residue was analyzed by ^1H NMR for identifying the organic products.

Reaction with HCl . Protolytic degradation was performed on all the σ -alkyl derivatives. The complexes (10 mg) were dissolved in 0.6 mL of CD_2Cl_2 , and gaseous HCl was bubbled through. The solution containing $\text{M}(\text{PNP})\text{Cl}_2$ and organic products was characterized by ^1H NMR spectroscopy.

X-ray Analysis. Crystal data and collection details for **2a-BF₄** are given in the Supporting Information. The most relevant bond distances and angles are reported in Table 1. Data collection was performed at 298 K on a Bruker-Nonius KappaCCD single-crystal diffractometer with monochromated $\text{Mo K}\alpha$ ($\lambda = 0.71073 \text{ \AA}$) radiation. Data were collected and integrated using the Bruker Nonius COLLECT software package,¹⁷ and a semiempirical absorption correction was applied (multiscan SADABS¹⁸). The structure was solved by direct methods and refined by the full matrix least-squares method on F^2 against all independent measured reflections (SHELX-97 package¹⁹). All non-hydrogen atoms were refined with anisotropic displacement parameters. H atoms were placed in

(17) *Collect*, Data collection software; Nonius BV: Amsterdam, 1997–2000.

(18) *SADABS*, area detector scaling and absorption correction; Bruker AXS, 2002

idealized positions and refined by a riding model with thermal parameters U_{iso} set to the U_{eq} of the carrier atoms. The light atoms in the molecule are affected by rather large thermal motion since it was not possible to collect data at low temperature. This accounts for low bond precision on some C–C bonds and for an average C–C ring (1.37 \AA) distance smaller than standard. The high value of R_{int} , greater than 0.10, may be ascribed to the not very high quality of crystals that were obtained only with great difficulty. One peak of residual electronic density larger than 1.0 e \AA^{-3} was found near the heavy atom, so it makes no chemical sense. For the graphical representation, ORTEP-III for Windows was used as implemented in the program system WinGX.²⁰

All crystallographic data have been deposited with the Cambridge Crystallographic Data Center (CCDC). The deposition number is CCDC 653493. These data can be obtained free of charge at www.ccdc.cam.ac.uk/conts/retrieving.html or from the Cambridge Crystallographic Data Centre, 12 Union Road, Cambridge CB2 1EZ, UK [fax: (internat.)+44-1223/336-033; e-mail: deposit@ccdc.cam.ac.uk].

Acknowledgment. This work was supported in part by MIUR (PRIN Grant No. 2004-030719). We thank the CIMCF, University of Napoli, for access to the NMR facilities and Miss Cinzia Barbato for experimental assistance.

Supporting Information Available: Crystallographic information file (CIF) for compound **2a-BF₄**. This material is available free of charge via the Internet at <http://pubs.acs.org>.

OM700692S

(19) Sheldrick, G. M. *SHELX97* [Includes *SHELXS97*, *SHELXL97*], Programs for Crystal Structure Analysis (Release 97-2); Institut für Anorganische Chemie der Universität: Göttingen, Germany, 1998.

(20) Farrugia, L. J. *WinGX*, Version 1.70.00, An Integrated System of Windows Programs for the Solution, Refinement and Analysis of Single-crystal X-Ray Diffraction Data. *J. Appl. Crystallogr.* **1999**, *32*, 837–838.